frontiers | Frontiers in Energy Research

ORIGINAL RESEARCH
published: 13 July 2022
doi: 10.3389/fenrg.2022.899771

Nacre-Like Reduced Graphene Oxide/Silver Nanowire Paper With Reinforced Chemical and Electrical Stability for Fast Electrical Heating System

Xiuxiu Zou[1], Kuizhong Shen[1], Yan Lin[1], Fangmin Liang[1], Enhui Sun[2], Yiqiang Wu[3] and Guigan Fang[1]**

[1]*Institute of Chemical Industry of Forest Products, CAF, Key Lab of Biomass Energy and Material, Jiangsu Province, Co-Innovation Center of Efficient Processing and Utilization of Forest Resources, National Engineering Lab for Biomass Chemical Utilization, Nanjing, China,* [2]*Key Laboratory of Saline-Alkali Soil Improvement and Utilization (CoastalSaline-AlkaliLands), Ministry of Agriculture and Rural Affairs, Jiangsu Collaborative Innovation Center for Solid Organic Waste Resource Utilization, Institute of Agricultural Resources and Environment, Jiangsu Academy of Agricultural Sciences, Jiangsu Province, Nanjing, China,* [3]*School of Materials Science and Engineering, Central South University of Forestry and Technology, Changsha, China*

OPEN ACCESS

Edited by:
Faming Wang,
Southeast University, China

Reviewed by:
Yang Li,
Hong Kong University of Science and Technology, Hong Kong, SAR China
Dusan Losic,
University of Adelaide, Australia

***Correspondence:**
Kuizhong Shen
kuizhong@icifp.cn
Guigan Fang
ppfangguigan@163.com

Specialty section:
This article was submitted to Process and Energy Systems Engineering, a section of the journal Frontiers in Energy Research

Received: *21 March 2022*
Accepted: *23 May 2022*
Published: *13 July 2022*

Citation:
Zou X, Shen K, Lin Y, Liang F, Sun E, Wu Y and Fang G (2022) Nacre-Like Reduced Graphene Oxide/Silver Nanowire Paper With Reinforced Chemical and Electrical Stability for Fast Electrical Heating System. Front. Energy Res. 10:899771. doi: 10.3389/fenrg.2022.899771

Silver nanowire (AgNW) has excellent thermal conductivity, which is an ideal material for fabricating flexible electrical heating materials. However, the poor stability of AgNWs is far from meeting the requirements for the practical application of electrical heating materials. Herein, by imitating the layered structure of nacre, the reduced graphene oxide (rGO)/AgNWs paper with a nacre-like structure was successfully prepared using a simple gravity-induced deposition approach. The obtained rGO/AgNWs paper showed excellent electrical conductivity (19.61 Ω/sq) and good pattern adjustability at the rGO to AgNWs ratio of 1:1. More importantly, the rGO/AgNWs paper exhibited high resistance to oxygen and water vapor, thus realizing long-term stability and reliability. Moreover, the design of a nacre-like structure could improve the thermal management performances of rGO/AgNWs paper, making it achieve a high Joule heating temperature (~215.83°C) at low supplied voltages (3 V), the rapid response time (~12 s) and long-term heating stability. These results indicate that the prepared rGO/AgNWs paper promises to be an electrical heating component with high chemical stability for thermal management electric materials.

Keywords: silver nanowire, nacre-like structure, reduced graphene oxide, chemical stability, thermal management performances

INTRODUCTION

Thermal management electric materials have been extensively used in various electronic devices due to excellent thermal conductivity and Joule heating performances, such as a solar cell (Tan et al., 2020), electronic displays (Sato et al., 2020), electromagnetic shielding instruments (Barani et al., 2020), and more. However, with the rapid development of wearable electronics and flexible electronics, the traditional thermal management electric materials, silicon, and indium tin oxid suffered from inherent brittleness, which seemed to be difficult to satisfy requirements for flexible

electronics (Kim et al., 2019; Wu et al., 2021; Yang et al., 2021). Therefore, the investigation of flexible conductive materials with excellent thermal management performances is of crucial importance. Recently, silver nanowire (AgNW) and graphene have attracted enormous attention and been widely applied in flexible thermal management electronics due to their high electrical conductivity and superior thermal conductivity (Chen J. et al., 2013; Kim D.-Y. et al., 2014; Yang et al., 2015; Jo et al., 2017). Bharat et al. prepared an AgNWs-graphene network by spin-coated method, which exhibited long-term stability and reliability for Joule heating performances. The result arose from bridging of AgNWs with graphene nanoplatelets, which provided additional electric channels, resulting in the enhancement of the thermal stability and mobility of carriers in the AgNWs-graphene network (Bharat et al., 2019). Thus, the AgNWs-graphene network is recognized as a highly promising thermal management electric material with good mechanical properties (Maize et al., 2015; Alotaibi et al., 2018; Bharat et al., 2019; Zhu et al., 2020). Unfortunately, AgNW is threatened by oxygen and heat and tends to oxidize rapidly or even resolve into small balls in the harsh environment, e.g., high temperature and damp heat, which limits its practical application for thermal management electric materials (Liu et al., 2018).

To date, designing a barrier structure to enhance the chemical stability of AgNWs is an effective way (Chen R. et al., 2013). There are two main strategies to achieve the barrier structure of AgNWs: 1) nonselective coating (Chae et al., 2020) and 2) selective wrapping (Huang et al., 2018). The latter strategy is based on the idea that the size of any material can be designed to guarantee mechanical flexibility, and thus provides a better solution to enhance the inoxidizability of the AgNWs (Li et al., 2020). Previous studies mainly concentrated on the combination of inert metal and AgNWs to avoid the corrosions of AgNWs in the air and at high temperatures. However, it is difficult to form the continuous and ultrathin inert metal layers on the surface of AgNWs (Niu et al., 2017; An et al., 2018). Graphene oxide (GO), a two-dimensional material, shows a compact structure, adjustable dimension, and abundant oxygen-containing functional groups, which is selectable wrapped material for AgNWs (Mehta et al., 2015; Hong et al., 2016; Wu et al., 2019). In recent years, a number of structures have been attempted to achieve the wrapping of GO to AgNWs, including core-shell structure (Yang et al., 2020), bridging structure (Qiao et al., 2020), and nacre structure (Meng et al., 2019). The nacre structure was known as high strength and high toughness, which could effectively improve the stress distribution and reinforce the mechanical/chemical stability (Wei and Xu, 2021). Therefore, the design of the nacre structure between GO and AgNWs has been widely explored, but the GO has poor electrical conductivity.

A previous study found that the reduction of GO could improve the electrical conductivity and thermal conductivity (Guex et al., 2017). Importantly, it could maintain intrinsic chemical stability. So far, researchers prefer to use hydrazine and hydrazine hydrate to fabricate the conductive reduced graphene oxide (rGO). Although the method could enhance the electrical conductivity and thermal conductivity of GO, there are still some defects that limit its application (Ren et al., 2011; Mahmudzadeh et al., 2019). First, toxic chemicals cause ever-growing environmental issues and potential experiment risks. Second, the rigorous reaction conditions display the great requirements for equipment (Zhou et al., 2019). Therefore, the fabrication of rGO remains a daunting challenge using an eco-friendly, secure, and low-cost method. Fortunately, the L-ascorbic acid (L-AA) is extensively found in natural plants and shows biocompatibility, non-toxic and low cost, which shows great potential for the reduction of GO. In addition, L-AA exhibits excellent reducibility and mild reaction conditions, allowing it to be a promising reducing agent for the reduction of GO (Zhang et al., 2010; Moretti et al., 2017; Njus et al., 2020).

To overcome the poor chemical stability of AgNWs, in this study, a nacre-like rGO/AgNWs composite material was successfully prepared by a simple gravity-induced deposition method. This method presented an alternative strategy without a high-temperature process or polluted reagent for the reduction of GO. The construction of nacre-like structures between rGO and AgNWs led to strong interface adhesion and continuous electrical path. The rGO/AgNWs paper showed outstanding electrical conductivity, flexible pattern adjustability, high inoxidizability, and good thermal management performances. The effects of reaction conditions including reaction temperature, reaction time, and the ratio of L-AA to GO on the reduction of GO were investigated detailedly. Meanwhile, the effects of rGO content on the electrical conductivity of rGO/AgNWs paper were also researched. The surface morphology of rGO/AgNWs paper was observed by SEM to confirm the distribution and compatibility of AgNWs in rGO. Furthermore, the rGO/AgNWs paper displayed excellent thermal management capabilities including high Joule heating temperature at low supplied voltages, rapid response time, sufficient heating stability, and reliability.

EXPERIMENTAL SECTION

Materials and Chemicals

Silver nitrate ($AgNO_3$), polyvinylpyrrolidone (PVP, MW = 360000), ethylene glycol (EG), sodium bromide, sodium chloride, ethanol, and acetone were purchased from Aladdin Chemistry Co. Ltd. (Shanghai, China). Graphene oxide (GO) was obtained from XFNANO Materials Technology Co., Ltd. (Nanjing, China). L-Ascorbic acid and ammonia solution was offered by Sinopharm Chemical Reagent Co. Ltd. (Shanghai, China).

Preparation of AgNWs and GO Solution

AgNWs were synthesized by the modified polyol method, which was reported in our previous work (Zou et al., 2022). Briefly, 0.2 g PVP was first dissolved in 30 ml EG solution and then stirred at RT. Afterward, 0.25 g $AgNO_3$ was added to the EG/PVP solution to obtain a transparent and homogeneous mixed solution under the condition of magnetic stirring. Subsequently, 1.10 g NaCl solution (0.01 wt% in EG) and 0.55 g NaBr solution (0.01 wt% in

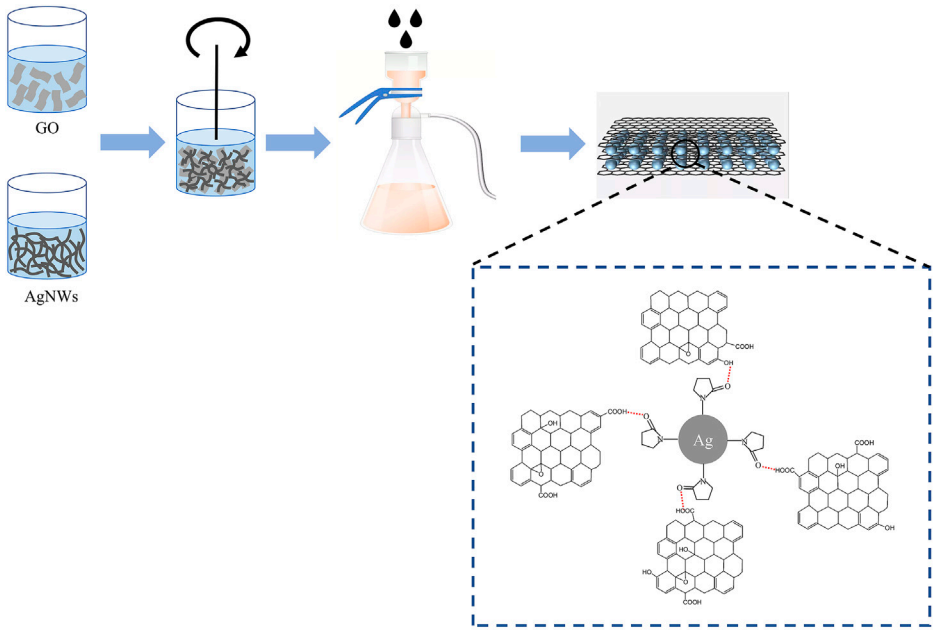

FIGURE 1 | Schematic illustration for the fabrication of rGO/AgNWs paper.

EG) were added to the mixture, then immediately placed into a reactor and allowed to stand at 160°C for 3 h. Finally, the solid was consecutively washed with ethanol and acetone by centrifugation of 4500 rpm for 7 min to remove the excess chemicals and the silver nanoparticles (AgNPs). The obtained AgNWs were diluted with ethanol to a concentration of 0.4 mg/ml before use.

10 mg GO was added to 100 ml ethanol and then transferred into broken series to treat for 1 h under the condition of ultrasonic wave. Afterward, the as-prepared GO solution was diluted with ethanol to a concentration of 0.1 mg/ml.

Preparation of rGO/AgNWs Paper

rGO/AgNWs paper was synthesized by a simple gravity-induced deposition method. 30 ml AgNWs solution was slowly added to the 120 ml GO solution under vigorous stirring to react for 2 h. Afterward, the GO/AgNWs solution was filtrated through a microporous membrane with a diameter of 0.22 μm, followed by rinsing with deionized (DI) water for 10 s to remove the residual ethanol solution. The obtained GO/AgNWs were re-dispersed in DI water. Similarly, we also fabricated other GO/AgNWs dispersion using the same method, but the addition of GO was changed to 240 and 360 ml to determine the effects of GO layers on electrical performance.

In this work, L-AA was used as the reducing agent to reduce the GO, which could effectively solve the problems of the traditional hydrazine and hydrazine hydrate method and maximally lowered the environmental pollution and the risk of toxic chemicals (Zhang et al., 2010). A series of rGO/AgNWs papers were manufactured by optimizing the reaction conditions including the reaction temperature, reaction time, and the ratio of GO and L-AA to evaluate the reduced properties of L-AA to GO. In detail, the L-AA was mixed with the GO/AgNWs solution, then the ammonia solution was slowly added to the mixture until the pH reached 10. Immediately, the mixed solution reacted at a high temperature. Afterward, the rGO/AgNWs were washed with DI water several times to remove the residual chemicals. Finally, the rGO/AgNWs solution was filtrated through a microporous membrane with a diameter of 0.22 μm to obtain the rGO/AgNWs paper and then placed into a 160°C thermocompressor with 0.88 MPa for 20 min, the schematic illustration of the fabrication of rGO/AgNWs paper is shown in **Figure 1**.

In addition, the pure AgNWs and rGO film were achieved using 30 ml AgNWs solution and 120 ml rGO solution by the same method, respectively.

Characterization

The surface morphology and elemental mapping analysis were observed by SU8100 scanning electron microscopy (SEM, FEI, United States) at 5.0 kV. The microstructure of AgNWs was obtained from a TF 20 transmission electron microscopy (TEM, FEI, United States) at 200 kV. The surface functional groups of AgNWs, GO, GO/AgNWs and rGO/AgNWs were characterized by 409 PC-iS10 Fourier transform infrared (FT-IR, Nestal, Germany). The X-ray diffraction (XRD, Bruker, Germany) characterization was carried out on a D8 Advanced diffractometer at 30 mA with a 40 kV Cu-Kα radiation, and the measurement of 2θ increased from 5° to 90° at a rate of 5°/min. The sheet resistance of rGO/AgNWs paper was measured by an M-6 four-point probe resistance tester (Anhui, China) with a tungsten probe gap of 2 mm and a probe radius of 40 μm. Raman spectra characterization was performed on a DXR532 laser Raman spectrometer (Thermo Fisher Scientific, United States) with an excitation light source of 532 nm. The surface temperature of rGO/AgNWs paper was recorded by a Fotric

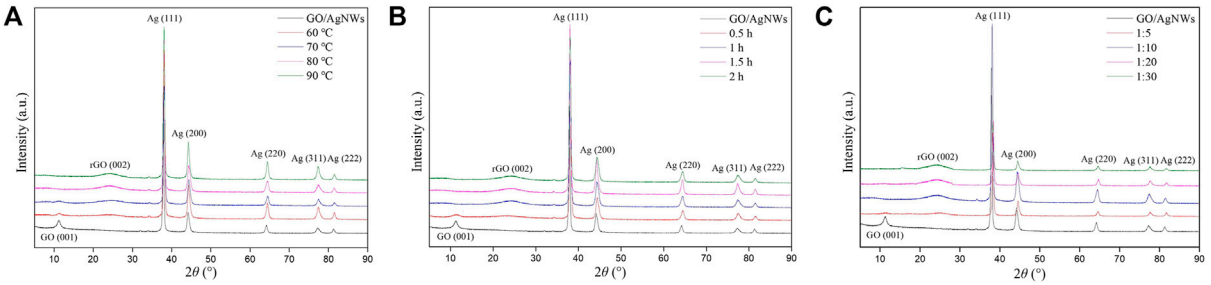

FIGURE 2 | XRD spectra of the reduced rGO/AgNWs paper at different reaction temperatures **(A)**, reaction time **(B)**, and the ratio of L-AA and GO **(C)**.

348 thermal imager (Shanghai. China). The data of the thermal imager was analyzed by an analyzer, and the IR emissivity was adjusted to 1 to avoid heat residues from other surrounding sources. The current-voltage (I-V) curves of rGO/AgNWs paper were recorded using an LW-K1003DC transformer (Hongkong, China).

RESULTS AND DISCUSSION

Effects of Reaction Conditions on the Reduction of GO

We characterized the XRD spectra of rGO/AgNWs to optimize the reduced conditions of GO, as shown in **Figure 2**. **Figure 2A** showed that the rGO/AgNWs were reduced by the different temperatures at a reaction time of 1 h and the ratio of GO to L-AA of 1:10. The XRD spectra of GO paper and rGO paper are shown in **Supplementary Figure S3**. It was clearly seen that a significant peak located at around 11.25° in the GO/AgNWs, which was indexed to the (001) crystal plane reflection of GO (Niu et al., 2017), and other diffraction peaks were observed at around 38.04°, 44.25°, 64.13°, 77.21°, and 81.40°, corresponding to the (111), (200), (220), (311), and (222) crystal planes of metallic silver, respectively (Xu et al., 2019). At a low reaction temperature of 60°C, there is a new diffraction peak at around 24.4°, originating from the (002) crystal plane reflection of graphite (Chen et al., 2018), which is attributed to the reduction of GO (Silva et al., 2018). In addition, the intensity of the (001) crystal plane became weaker and even disappearance as the temperature increased from 60 to 80°C. It is worth noting that the rGO/AgNWs exhibit similar diffraction peaks of metallic silver with GO/AgNWs, indicating that the reduction of GO was not influencing the crystal structure of AgNWs (Chen J. et al., 2013). In addition, the Ag (200) peaks slightly shifted to larger angles in the XRD spectra of rGO/AgNWs. It is because the rGO/AgNWs paper suffered thermocompression, resulting in low indices of lattice plane.

Figure 2B showed that the rGO/AgNWs were reduced by different reaction times at a reaction temperature of 80 °C and the ratio of GO to L-AA of 1:10. At the reaction time of 0.5 h, the intensity of the (001) crystal plane of GO was decreased and the new peak of the (002) crystal plane was presented, suggesting that partial oxygen functional groups of GO were removed (Xiang et al., 2020). With the increase of reaction time (1 h), the (001) crystal plane of GO was not observed. On the contrary, the intensity of the (002) crystal plane increased. When the further increase of reaction time, the diffraction peaks were changed barely.

The content of L-AA was an important factor in the reduction of GO (Guardia et al., 2010). **Figure 2C** showed that the rGO/AgNWs were reduced by different ratios of GO to L-AA at a reaction temperature of 80°C and reaction time of 1 h. At the ratio of GO to L-AA of 1:5, the intensity of the (001) crystal plane became weaker compared with GO/AgNWs. In addition, a new broad peak was shown in the XRD pattern, that corresponded to the (002) crystal plane of graphite. The result indicates that the GO was reduced poorly to graphite. With the increase in the ratio of GO to L-AA (1:10), the (001) crystal plane was not presented in the XRD pattern of rGO/AgNWs, which was caused by the complete reduction of GO. Meanwhile, the intensity of the (002) crystal plane increased significantly. These results confirm that GO was well reduced to rGO as the ratio of GO to L-AA of 1:10.

Structural Characterization of rGO/AgNWs Paper

It has been known from the aforementioned XRD results that L-AA could reduce GO efficiently. Therefore, the Raman spectra of the AgNWs, GO, GO/AgNWs paper and rGO/AgNWs paper were characterized to further demonstrate the reduction of GO. The GO showed the D band peak and G band peak, that was attributed to the inherent defects or disorders in carbon and the phonon vibration of sp^2-hybridized carbon with E_{2g} symmetry, respectively (Ferrari and Robertson, 2000). Generally, the intensity ratio value of the D band peak to the G band peak (I_D/I_G) was used to evaluate the structural disorder within graphene lattices, which further expressed the degree of reduction of GO (Yang et al., 2020). As shown in **Figure 3A**, there is no Raman diffraction peak in AgNWs. In contrast, the D band peak at 1360.88 cm^{-1} and the G band peak at 1599.81 cm^{-1} were observed in the Raman spectrum of GO. In addition, the I_D/I_G of GO was 0.98, and the I_D/I_G barely changed in the GO/AgNWs paper. Compared to the pure GO and GO/AgNWs paper, the rGO/AgNWs paper exhibited lower I_D/I_G (~0.55), which was attributed that the inherent defects of the D band peak being relatively less (Kim S. H. et al., 2014).

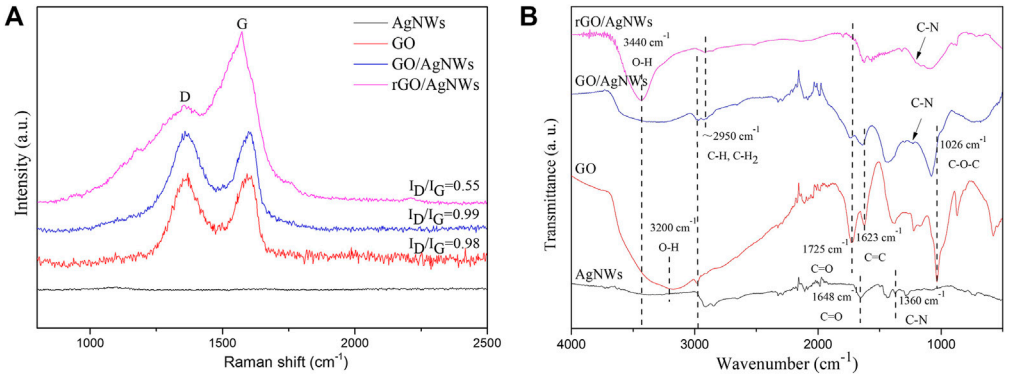

FIGURE 3 | Raman spectra **(A)** and FT-IR spectra **(B)** of AgNWs, GO, GO/AgNWs paper, and rGO/AgNWs paper.

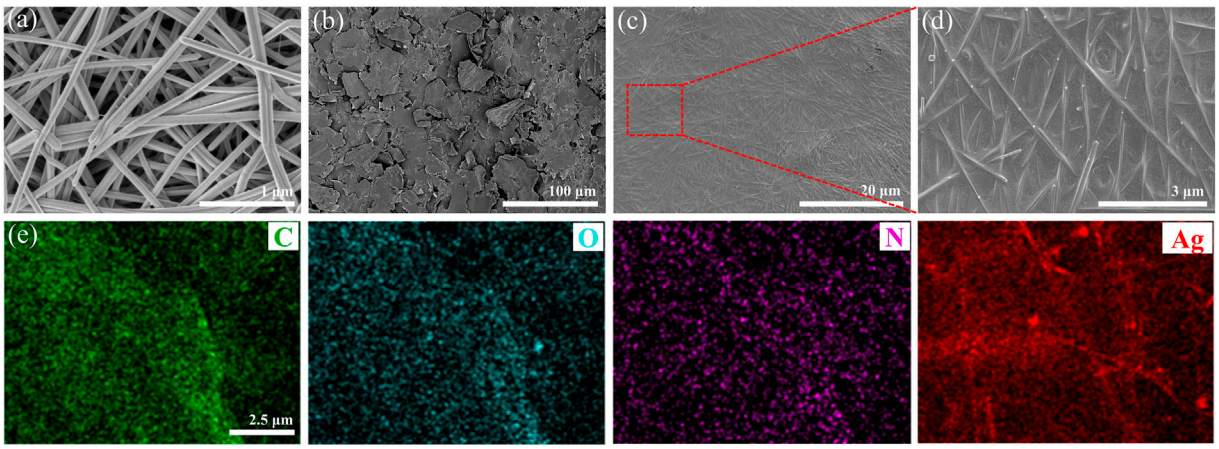

FIGURE 4 | SEM images of AgNWs **(A)**, GO **(B)**, and rGO/AgNWs paper **(C,D)**, target element mapping of rGO/AgNWs paper **(E)**.

To characterize the surface chemistry and identify possible interfacial interactions between AgNWs and rGO, FTIR analysis was employed (**Figure 3B**). FTIR spectrum of the AgNWs displayed the typical peaks at 1360 cm^{-1}, 1648 cm^{-1}, 2845 cm^{-1}, 2921 cm^{-1}, and 3200 cm^{-1}, corresponding to the stretching vibration of the C-N group, C=O group, CH_2 group, CH group, and OH group, respectively (Jiang et al., 2004). These groups resulted from the PVP wrapped in the surface of AgNWs. FTIR spectrum of GO showed clearly the vibration at 1026 cm^{-1} (stretching vibration of C-O-C group), 1623 cm^{-1} (stretching vibration of C-C group), 1725 cm^{-1} (stretching vibration of C=O group), and 3200 cm^{-1} (stretching vibration of OH group), which was similar with previous results (Wojtoniszak and Mijowska, 2012; Raucci et al., 2017). Compared with the FTIR spectra of GO and AgNWs, the C-O-C group, C=O group, and OH group of GO/AgNWs shifted to 1077 cm^{-1},1737 cm^{-1}, and 3440 cm^{-1}, respectively, which indicated the formation of hydrogen bonds between AgNWs and GO (Wan et al., 2021). After the reduction of GO, the relative intensity of the stretching vibration of the C=O group showed a decreasing trend and the stretching vibration of the C-O-C group was barely observed, which was attributed to the reduction of GO.

Morphology of rGO/AgNWs Paper

Figure 4 displays the micro-morphology of AgNWs, GO and rGO/AgNWs, and element distribution of rGO/AgNWs. The SEM image of AgNWs is shown in **Figure 4A**, it can be seen that the AgNWs obtained by the traditional polyol method possessed a long wire microstructure with a smooth surface. In addition, AgNWs exhibited a uniform morphology and no AgNPs were observed, indicating the high yield of AgNWs during the preparation process. As shown in **Supplementary Figure S1**, the surface of AgNWs was uniformly covered by a PVP layer with a thickness of 4.5 nm, which effectivity prevented the self-accumulation of AgNWs, and the result was consistent with a previous study (Liang et al., 2020). The SEM image of **Figure 4B** showed that GO was a two-dimensional nanosheet and no cracks or defects could be seen on the surface of GO. The GO exhibited abundant oxygen-containing functional groups, that could form strong hydrogen bonding interactions with the PVP layer covered on the surface of AgNWs. As a result, AgNWs conductive

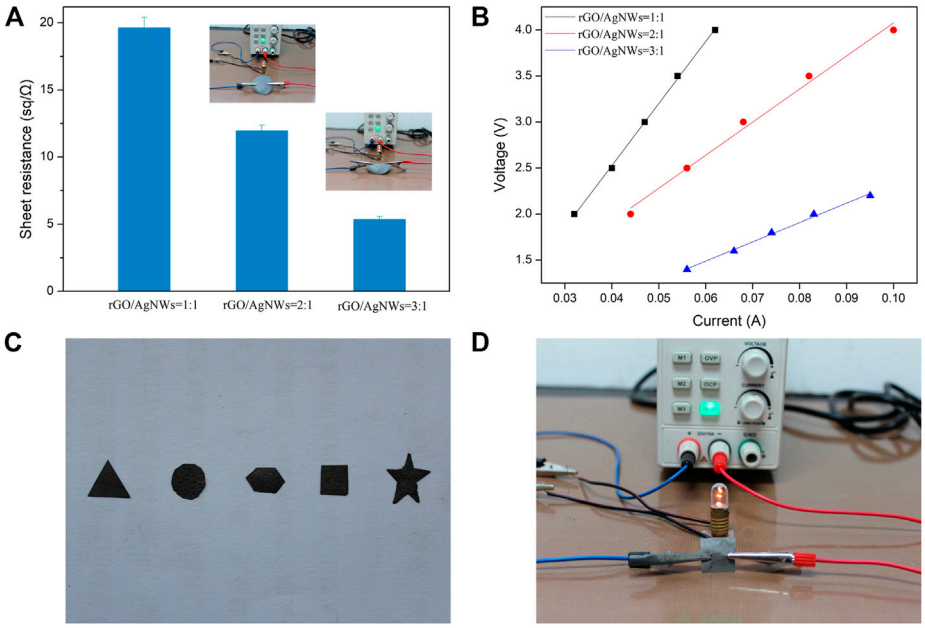

FIGURE 5 | Sheet resistance **(A)** and I-V curve **(B)** of rGO/AgNWs paper, the different patterns of rGO/AgNWs paper **(C)** and a digital photograph of the lighted LED lamp of patterned rGO/AgNWs paper **(D)**.

network was covered by GO to form the laminated nacre-like structure (**Figures 4C,D**). Apparently, this result signifies that the oxidation of AgNWs could be reduced. It is worth noting that the conductive network of AgNWs and the lamellar structure of rGO were well-preserved in rGO/AgNWs paper, guaranteeing excellent electrical conductivity. In addition, the elemental mapping also showed that the four elements of C, N, O, and Ag were uniformly distributed in rGO/AgNWs paper (**Figure 4E** and **Supplementary Figure S2**), indicating a good combination between AgNWs and rGO.

Electrical Property of rGO/AgNWs Paper

The electrical property of rGO/AgNWs paper was probed systematically, as shown in **Figure 5**. The sheet resistance of rGO/AgNWs paper could be tailored by increasing the content of rGO and AgNWs. The electrical property of rGO/AgNWs paper with different content of rGO is demonstrated in **Figure 5A**. At the rGO to AgNWs ratio of 1:1, the sheet resistance of rGO/AgNWs paper was 19.61 Ω/sq. Such superior electrical property was attributed to the inherent high conductivity of AgNWs and continuous conductive networks in the rGO layers (**Figures 4C,D**). However, it can be seen from **Supplementary Figure S4** that the rGO paper exhibited a higher sheet resistance (38.12 Ω/sq) than the rGO/AgNWs paper, which was due to the low inherent electrical conductivity of rGO. On the contrary, the AgNWs paper had a low sheet resistance of 1.01 Ω/sq, which was caused by the high electrical conductivity of metallic Ag. When the rGO to AgNWs ratio was increased to 2:1, the sheet resistance of rGO/AgNWs paper showed a significant decline, which was lower than 12 Ω/sq. In addition, the sheet resistance of rGO/AgNWs paper reduced continuously with the further increase of the ratio of rGO to AgNWs, which could be explained by the increasing conductive networks between rGO and AgNWs and the formation of more conductive rGO layers (Zheng et al., 2020). These results demonstrated that the electrical conductivity of the rGO/AgNWs paper increased unceasingly with the increase of the ratio of rGO to AgNWs. Meanwhile, the rGO/AgNWs paper was connected with a light emitting diode (LED) lamp to further verify its electrical property. It can be clearly seen that the rGO/AgNWs paper prepared with different content of rGO could successfully light up a LED lamp (see the insets of **Figure 5A**). The near-linear I-A curves of the rGO/AgNWs paper are shown in **Figure 5B**. According to Ohms law of the series circuit, we could directly obtain the sheet resistance from the slope of the I-A curve. It is can be seen that the sheet resistance became smaller when the decrease of voltage gradient (Murdani and Sumarli, 2019; Li et al., 2022). At the rGO to AgNWs ratio of 3:1, the rGO/AgNWs paper had the lowest sheet resistance than other rGO/AgNWs papers, which could achieve better conductive property and thermal conductive properties. The patterned design was also a critical factor for electronic devices (Myung et al., 2007). To confirm the shape flexibility of rGO/AgNWs paper, the photos of the patterned rGO/AgNWs paper are shown in **Figure 5C**. The rGO/AgNWs paper with five different shapes (*i.e.* triangle, circle, rhombus, square, and star) was prepared successfully by cutting the rGO/AgNWs paper. More importantly, the surface of the patterned rGO/AgNWs paper was complete without defects such as ruptures and collapse. This result was attributed to the excellent interface connection between rGO and AgNWs (Wei and Xu, 2021). It is worth noting that the rGO/AgNWs paper could successfully light up a LED lamp in different patterned shapes, demonstrating that the rGO/

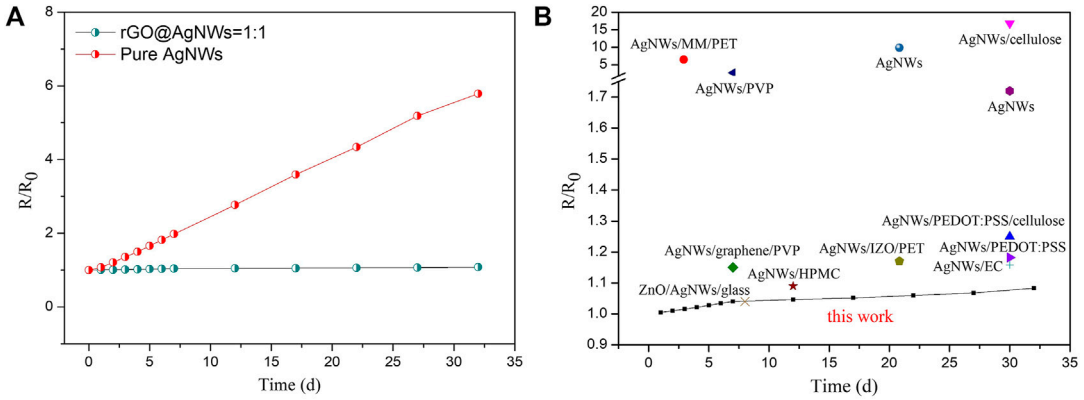

FIGURE 6 | The R/R_0 variations of rGO@AgNWs paper and pure AgNWs film versus time at air **(A)**, comparison of the antioxidation property of rGO@AgNWs paper with other AgNWs composite materials **(B)**.

AgNWs paper could serve as an electrode for lightening LED under different shaped environments.

Antioxygenic Property of rGO/AgNWs Paper

Long-term chemical stability is an important factor for thermal management of electric materials in commercial application, but the AgNWs tend to oxidize in the air (Yang et al., 2020). Herein, the nacre-like structure of rGO/AgNWs paper was designed to improve the antioxygenic property of AgNWs. The ratio of original sheet resistance to current sheet resistance (R/R_0) variations of rGO/AgNWs paper and pure AgNWs film versus time at air were compared, which is displayed in **Figure 6**. The rGO/AgNWs paper and pure AgNWs film were exposed to air for 32 d and the temperature and humidity were 25°C and 50%, respectively. As shown in **Figure 6A**, the R/R_0 value of pure AgNWs film increased from 1 to 1.98 after exposure to air for 7 days, indicating the poor antioxygenic property. In contrast, the R/R_0 value of the rGO/AgNWs paper increased from 1 to 1.04 after exposure to air for 7 days, suggesting that the rGO/AgNWs paper exhibited higher stability than pure AgNWs paper. After continuous exposure to air for 25 days, the sheet resistance of rGO/AgNWs paper increased slightly, which strongly demonstrated that the rGO/AgNWs paper possessed high conductive stability in air. The result was attributed that the gas-impermeable rGO layer avoided the corrosions of oxygen to AgNWs (Yang et al., 2020). However, the R/R_0 value of pure AgNWs film increased to 5.79 after exposure for 25 days in the same environment, suggesting that the conductive AgNWs network was destroyed in the air. To highlight the antioxygenic property of the rGO/AgNWs paper, the antioxygenic property of previously studied AgNWs composite materials were summarized comprehensively (**Figure 6B**). The R/R_0 value of the rGO/AgNWs paper was increased to 1.08 after exposure to air for 32 days, which outperformed most of the currently AgNWs conductive composite materials by far (Ferrari and Robertson, 2000; Lee et al., 2013; Zhang et al., 2014; Zhang et al., 2014; Shin et al., 2018; Shinde et al., 2018; Xiong et al., 2018; Liu et al., 2021).

Thermal Management Properties of rGO/AgNWs Paper

Herein, the rGO/AgNWs paper has widespread application in heating electronic devices that require temperature regulation, such as heating elements, micro-wave ovens, and so on (Song et al., 2018; Hu et al., 2020). Thermal management materials also could control their own temperatures under high temperature and large operating voltage conditions, that is, Joule heating performances, in addition to excellent electrical conductivity and shaped flexibility (Liang et al., 2020). We propose that the rGO/AgNWs paper could provide both excellent thermal stability and high electrical heating temperature.

Figure 7A shows the temperature variations of different rGO/AgNWs paper versus time at the applied voltage of 2 V. Generally, a good electronic conductor was also a superior thermal conductor (Manno et al., 2012). At the ratio of rGO to AgNWs of 1:1, the temperature of rGO/AgNWs paper increased rapidly at the beginning, followed by a slow increase, and finally reached a balanced temperature of 117.90°C at 32 s, indicating that the nacre-like structure of the rGO/AgNWs paper could form the excellent heat conductive paths. When the power was cut off, the temperature of rGO/AgNWs paper dropped back to room temperature at a high rate. The balance temperature of the rGO/AgNWs paper increased with the increase of the ratio of rGO to AgNWs, and the balance temperature of the rGO/AgNWs paper was elevated to the highest value of 216.57°C at the rGO to AgNWs ratio of 3:1. Such excellent electrical heating temperature of the rGO/AgNWs paper could be explained as follows. First, the gas-impermeable rGO hindered effectively the permeation of heat into the outer environment under an environment of low temperature or humidity. Second, the synergistic effects between rGO and AgNWs could improve the current-carrying capacity, and further increased the Joule heating temperature of rGO/AgNWs paper (Yang et al., 2020). To verify the latter, the temperature variations of rGO/AgNWs paper versus time at different applied voltage was recorded, as shown in **Figure 7B**. It is clearly seen that the Joule heating temperature of rGO/

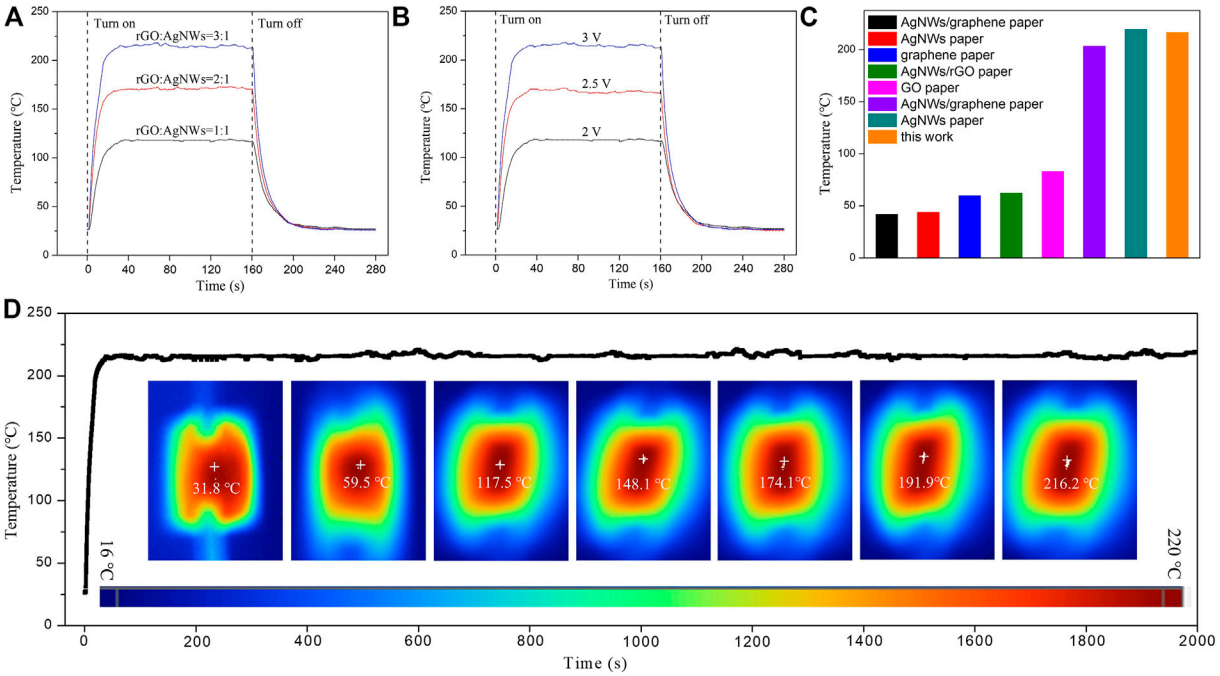

FIGURE 7 | The surface temperature variations of rGO/AgNWs paper with different rGO content versus time at an applied voltage of 2 V **(A)**, the surface temperature variations of rGO/AgNWs paper versus time at a voltage of 2 V, 2.5 and 3 V **(B)**, comparison of the Joule heating temperature of as-prepared rGO/AgNWs paper with other composite papers **(C)**, the time-temperature curve of rGO/AgNWs paper at an applied voltage of 3 V **(D)**.

AgNWs paper increased incrementally with the increase of applied voltage. At applied voltages of 2 V, 2.5, and 3 V, the rGO/AgNWs paper achieved maximum temperatures of 117.90°C, 168.42°C, and 217.22°C, respectively. The Joule heating temperature was almost positively correlated with the increase of rGO content and applied voltage, which verified the synergy of rGO and AgNWs in the construction of electrical and thermal networks. Moreover, when the applied voltage increased in gradient, the Joule heating temperature of the rGO/AgNWs paper responded quickly without significant hysteresis, which suggested that the rGO/AgNWs paper had great application potential in the field of intelligent temperature control (Nan et al., 2020). To the best of our knowledge, the rGO/AgNWs paper presented a higher Joule heating temperature at low applied voltage than most other thermal conductors (Chung et al., 2018; Bharat et al., 2019; Dai et al., 2019; Kim et al., 2020; Nan et al., 2020; Yang et al., 2020; Yang et al., 2020; Liu et al., 2022). In order to evaluate the long-term stability and reliability of the rGO/AgNWs paper, the temperature variations versus time at a constant applied of 3 V were characterized, as shown in **Figure 7D**. The rGO/AgNWs paper exhibited a stable Joule heating temperature of ~215.83°C within 2000 s, indicating that the rGO/AgNWs paper could achieve stability and reliability under long-term operating conditions. It is worth noting that the distribution of Joule heat was uniform on the surface of rGO/AgNWs paper. The above-mentioned results showed that the rGO/AgNWs paper displayed excellent Joule heat property, rapid response time, and long-term heating stability, which was promised to be applied to cutting-edge industrial fields, such as wearable thermal devices, artificial intelligence, and controllable heating elements.

CONCLUSIONS

In summary, based on the compact "brick-mud" structure of the nacre structure, we have proposed a novel structure to prepare rGO/AgNWs conductive paper. A simple gravity-induced deposition approach was used to construct the rGO/AgNWs paper with a nacre-like structure. The rGO/AgNWs paper could form strong interface adhesion and continuous electrical paths. In detail, the reduction conditions of GO were first optimized, and it is found that the GO could be well reduced to rGO at 80°C and the ratio of rGO to L-AA of 1:10 for 1 h. The microtopography, electrical conductivity, antioxygenic property, mechanical property, and thermal management performances of rGO/AgNWs paper were further investigated in detail. Results show that the distribution of AgNWs conductive network was improved due to the formation of nacre structure between rGO and AgNWs, and thus the rGO/AgNWs paper exhibited a low sheet resistance of 19.61 Ω/sq at the ratio of rGO to AgNWs of 1:1. In addition, the rGO/AgNWs paper had excellent pattern adjustability. Because of the design of the nacre structure of rGO/AgNWs paper, the rGO/AgNWs paper showed long-term conductive stability and reliability in the air, which was attributed that the gas-impermeable rGO layer avoiding the entry of oxygen and water vapor. In addition to these, the rGO/AgNWs paper also presented superior thermal management performances including high Joule heating temperature (~215.83°C) at low supplied voltages (3 V), the rapid response time (~12 s), and long-

term heating stability (~2000 s), indicating its security and reliability in practical application. The nacre-like composite materials with excellent barrier performance, easy operation, and low cost has extensive-ranging process compatibility, thus making it a potential method for fabricating other high-performance composite materials, such as solar display and OLED devices.

DATA AVAILABILITY STATEMENT

The original contributions presented in the study are included in the article/**Supplementary Material**; further inquiries can be directed to the corresponding author.

AUTHOR CONTRIBUTIONS

XZ: conceived and designed the study. KS: revising the manuscript. YL: conducting ES analysis. FL: interpretation of results. ES: idea of the work and revising the manuscript. YW: idea of the work and revising the manuscript. GF: idea of the work and interpretation of results.

FUNDING

This work was supported by the Jiangsu Province Agricultural Independent Innovation Fund [Grant Number: CX (19)2003], the National Natural Science Foundation of China (Grant Number: 31890771), and the Natural Science Foundation of Jiangsu Province (Grant Number: BK20211025).

SUPPLEMENTARY MATERIAL

The Supplementary Material for this article can be found online at: https://www.frontiersin.org/articles/10.3389/fenrg.2022.899771/full#supplementary-material

REFERENCES

Alotaibi, F., Tung, T. T., Nine, M. J., Coghlan, C. J., and Losic, D. (2018). Silver Nanowires with Pristine Graphene Oxidation Barriers for Stable and High Performance Transparent Conductive Films. *ACS Appl. Nano Mat.* 1, 2249–2260. doi:10.1021/acsanm.8b00255

An, S., Kim, Y. I., Jo, H. S., Kim, M.-W., Swihart, M. T., Yarin, A. L., et al. (2018). Oxidation-resistant Metallized Nanofibers as Transparent Conducting Films and Heaters. *Acta Mater.* 143, 174–180. doi:10.1016/j.actamat.2017.09.068

Barani, Z., Kargar, F., Mohammadzadeh, A., Naghibi, S., Lo, C., Rivera, B., et al. (2020). Multifunctional Graphene Composites for Electromagnetic Shielding and Thermal Management at Elevated Temperatures. *Adv. Electron. Mat.* 6, 2000520–2000532. doi:10.1002/aelm.202000520

Bharat, S., Jun-Sik, K., and Ashutosh, S. (2019). AgNWs-graphene Transparent Conductor for Heat and Sensing Applications. *Mat. Res. Express* 6, 1–21.

Chae, W. H., Sannicolo, T., and Grossman, J. C. (2020). Double-Sided Graphene Oxide Encapsulated Silver Nanowire Transparent Electrode with Improved Chemical and Electrical Stability. *ACS Appl. Mat. Interfaces* 12, 17909–17920. doi:10.1021/acsami.0c03587

Chen, J., Bi, H., Sun, S., Tang, Y., Zhao, W., Lin, T., et al. (2013a). Highly Conductive and Flexible Paper of 1D Silver-Nanowire-Doped Graphene. *ACS Appl. Mat. Interfaces* 5, 1408–1413. doi:10.1021/am302825w

Chen, R., Das, S. R., Jeong, C., Khan, M. R., Janes, D. B., and Alam, M. A. (2013b). Co-Percolating Graphene-Wrapped Silver Nanowire Network for High Performance, Highly Stable, Transparent Conducting Electrodes. *Adv. Funct. Mat.* 23, 5150–5158. doi:10.1002/adfm.201300124

Chung, W.-H., Park, S.-H., Joo, S.-J., and Kim, H.-S. (2018). UV-assisted Flash Light Welding Process to Fabricate Silver Nanowire/graphene on a PET Substrate for Transparent Electrodes. *Nano Res.* 11, 2190–2203. doi:10.1007/s12274-017-1837-3

Dai, W., Lv, L., Lu, J., Hou, H., Yan, Q., Alam, F. E., et al. (2019). A Paper-like Inorganic Thermal Interface Material Composed of Hierarchically Structured Graphene/Silicon Carbide Nanorods. *ACS Nano* 13, 1547–1554. doi:10.1021/acsnano.8b07337

Fernández-Merino, M. J., Guardia, L., Paredes, J. I., Villar-Rodil, S., Solís-Fernández, P., Martínez-Alonso, A., et al. (2010). Vitamin C Is an Ideal Substitute for Hydrazine in the Reduction of Graphene Oxide Suspensions. *J. Phys. Chem. C* 114, 6426–6432. doi:10.1021/jp100603h

Ferrari, A. C., and Robertson, J. (2000). Interpretation of Raman Spectra of Disordered and Amorphous Carbon. *Phys. Rev. B* 61, 14095–14107. doi:10.1007/BF0254369210.1103/physrevb.61.14095

Guex, L. G., Sacchi, B., Peuvot, K. F., Andersson, R. L., Pourrahimi, A. M., Ström, V., et al. (2017). Experimental Review: Chemical Reduction of Graphene Oxide (GO) to Reduced Graphene Oxide (rGO) by Aqueous Chemistry. *Nanoscale* 9, 9562–9571. doi:10.1039/x0xx0000010.1039/c7nr02943h

Hong, J.-Y., Kim, W., Choi, D., Kong, J., and Park, H. S. (2016). Omnidirectionally Stretchable and Transparent Graphene Electrodes. *ACS Nano* 10, 9446–9455. doi:10.1021/acsnano.6b04493

Hu, R., Liu, Y., Shin, S., Huang, S., Ren, X., Shu, W., et al. (2020). Emerging Materials and Strategies for Personal Thermal Management. *Adv. Energy Mat.* 10, 1903921–1903923. doi:10.1002/aenm.201903921

Huang, S., Zhang, Q., Li, P., Ren, F., Yurtsever, A., and Ma, D. (2018). High-Performance Suspended Particle Devices Based on Copper-Reduced Graphene Oxide Core-Shell Nanowire Electrodes. *Adv. Energy Mat.* 8, 1703658–1703668. doi:10.1002/aenm.201703658

Jiang, P., Li, S.-Y., Xie, S.-S., Gao, Y., and Song, L. (2004). Machinable Long PVP-Stabilized Silver Nanowires. *Chem. Eur. J.* 10, 4817–4821. doi:10.1002/chem.200400318

Kim, D.-Y., Sinha-Ray, S., Park, J.-J., Lee, J.-G., Cha, Y.-H., Bae, S.-H., et al. (2014a). Self-healing Reduced Graphene Oxide Films by Supersonic Kinetic Spraying. *Adv. Funct. Mat.* 24, 4986–4995. doi:10.1002/adfm.201400732

Kim, K., Park, Y. G., Hyun, B. G., Choi, M., and Park, J. U. (2019). Recent Advances in Transparent Electronics with Stretchable Forms. *Adv. Mater.* 31, 1804690–1804710. doi:10.1002/adma.201804690

Kim, S. H., Song, W., Jung, M. W., Kang, M.-A., Kim, K., Chang, S.-J., et al. (2014b). Carbon Nanotube and Graphene Hybrid Thin Film for Transparent Electrodes and Field Effect Transistors. *Adv. Mat.* 26, 4247–4252. doi:10.1002/adma.201400463

Kim, T.-G., Park, C.-W., Woo, D.-Y., Choi, J., and Yoon, S. S. (2020). Efficient Heat Spreader Using Supersonically Sprayed Graphene and Silver Nanowire. *Appl. Therm. Eng.* 165, 114572. doi:10.1016/j.applthermaleng.2019.114572

Lee, H. J., Hwang, J. H., Choi, K. B., Jung, S.-G., Kim, K. N., Shim, Y. S., et al. (2013). Effective Indium-Doped Zinc Oxide Buffer Layer on Silver Nanowires for Electrically Highly Stable, Flexible, Transparent, and Conductive Composite Electrodes. *ACS Appl. Mat. Interfaces* 5, 10397–10403. doi:10.1021/am4025802

Li, D., Wang, L., Ji, W., Wang, H., Yue, X., Sun, Q., et al. (2021). Embedding Silver Nanowires into a Hydroxypropyl Methyl Cellulose Film for Flexible Electrochromic Devices with High Electromechanical Stability. *ACS Appl. Mat. Interfaces* 13, 1735–1742. doi:10.1021/acsami.0c16066

Li, L., Li, W., Tong, K., Jiu, J., and Suganuma, K. (2020). Intense Pulsed Light-Induced Structure-Transformed Ultrathin Ni Shell for Improving the Chemical, Thermal, and Electrical Reliability of Metal Nanowire Electrodes without Transmittance Loss. *Chem. Eng. J.* 390, 124517. doi:10.1016/j.cej.2020.124517

Li, X., Jiang, W., Li, W., and Zhang, W. (2022). Effect of Carbon Content on Shielding and Mechanical Properties of Bamboo Charcoal/HDPE Composited. *J. For. Eng.* 7, 130–136.

Liang, C., Ruan, K., Zhang, Y., and Gu, J. (2020). Multifunctional Flexible Electromagnetic Interference Shielding Silver Nanowires/Cellulose Films with Excellent Thermal Management and Joule Heating Performances. *ACS Appl. Mat. Interfaces* 12, 18023–18031. doi:10.1021/acsami.0c04482

Liu, G.-S., Xu, Y., Kong, Y., Wang, L., Wang, J., Xie, X., et al. (2018). Comprehensive Stability Improvement of Silver Nanowire Networks via Self-Assembled Mercapto Inhibitors. *ACS Appl. Mat. Interfaces* 10, 37699–37708. doi:10.1021/acsami.8b13329

Liu, H., Huang, Z., Chen, T., Su, X., Liu, Y., and Fu, R. (2022). Construction of 3D MXene/Silver Nanowires Aerogels Reinforced Polymer Composites for Extraordinary Electromagnetic Interference Shielding and Thermal Conductivity. *Chem. Eng. J.* 427, 131540. doi:10.1016/j.cej.2021.131540

Mahmudzadeh, M., Yari, H., Ramezanzadeh, B., and Mahdavian, M. (2019). Highly Potent Radical Scavenging-Anti-Oxidant Activity of Biologically Reduced Graphene Oxide Using Nettle Extract as a Green Bio-Genic Amines-Based Reductants Source Instead of Hazardous Hydrazine Hydrate. *J. Hazard. Mater.* 371, 609–624. doi:10.1016/j.jhazmat.2019.03.046

Maize, K., Das, S. R., Sadeque, S., Mohammed, A. M. S., Shakouri, A., Janes, D. B., et al. (2015). Super-Joule Heating in Graphene and Silver Nanowire Network. *Appl. Phys. Lett.* 106, 143104–143110. doi:10.1063/1.4916943

Manno, M., Wang, P., and Bar-Cohen, A. (2012). Transient Thermoelectric Self-Cooling of a Germanium Hotspot. *Intersoc. Conf. Therm. Thermomechanical Phenom. Electron. Syst. ITHERM* 12, 413–420. doi:10.1109/ITHERM.2012.6231460

Mehta, R., Chugh, S., and Chen, Z. (2015). Enhanced Electrical and Thermal Conduction in Graphene-Encapsulated Copper Nanowires. *Nano Lett.* 15, 2024–2030. doi:10.1021/nl504889t

Meng, X., Zhao, S., Zhang, Z., Zhang, R., Li, J., Leng, J., et al. (2019). Nacre-inspired Highly Stretchable Piezoresistive Cu-Ag Nanowire/graphene Synergistic Conductive Networks for Strain Sensors and beyond. *J. Mat. Chem. C* 7, 7061–7072. doi:10.1039/c9tc00943d

Moretti, M., Fraga, D. B., and Rodrigues, A. L. S. (2017). Preventive and Therapeutic Potential of Ascorbic Acid in Neurodegenerative Diseases. *CNS Neurosci. Ther.* 23, 921–929. doi:10.1111/cns.12767

Murdani, E., and Sumarli, S. (2019). Student Learning by Experiment Method for Analyzing the Dynamic Electrical Circuit and its Application in Daily Life. *J. Phys. Conf. Ser.* 1153, 012119. doi:10.1088/1742-6596/1153/1/012119

Myung, D., Koh, W., Bakri, A., Zhang, F., Marshall, A., Ko, J., et al. (2007). Design and Fabrication of an Artificial Corneal Scaffold using Photolithographically Patterned Photopolymerized Hydrogel Construct. *Biomed. Microdevices* 9, 911–922. doi:10.1007/s10544-006-9040-4

Nan, B., Wu, K., Qu, Z., Xiao, L., Xu, C., Shi, J., et al. (2020). A Multifunctional Thermal Management Paper Based on Functionalized Graphene Oxide Nanosheets Decorated with Nanodiamond. *Carbon* 161, 132–145. doi:10.1016/j.carbon.2020.01.056

Niu, Z., Cui, F., Yu, Y., Becknell, N., Sun, Y., Khanarian, G., et al. (2017). Ultrathin Epitaxial Cu@Au Core-Shell Nanowires for Stable Transparent Conductors. *J. Am. Chem. Soc.* 139, 7348–7354. doi:10.1021/jacs.7b02884

Njus, D., Kelley, P. M., Tu, Y.-J., and Schlegel, H. B. (2020). Ascorbic Acid: The Chemistry Underlying its Antioxidant Properties. *Free Radic. Biol. Med.* 159, 37–43. doi:10.1016/j.freeradbiomed.2020.07.013

Qiao, Y., Wang, Y., Jian, J., Li, M., Jiang, G., Li, X., et al. (2020). Multifunctional and High-Performance Electronic Skin Based on Silver Nanowires Bridging Graphene. *Carbon* 156, 253–260. doi:10.1016/j.carbon.2019.08.032

Raucci, M. G., Giugliano, D., Longo, A., Zeppetelli, S., Carotenuto, G., and Ambrosio, L. (2017). Comparative Facile Methods for Preparing Graphene Oxide-Hydroxyapatite for Bone Tissue Engineering. *J. Tissue Eng. Regen. Med.* 11, 2204–2216. doi:10.1002/term.2119

Ren, P.-G., Yan, D.-X., Ji, X., Chen, T., and Li, Z.-M. (2011). Temperature Dependence of Graphene Oxide Reduced by Hydrazine Hydrate. *Nanotechnology* 22, 055705. doi:10.1088/0957-4484/22/5/055705

Sato, K., Tominaga, Y., and Imai, Y. (2020). Nanocelluloses and Related Materials Applicable in Thermal Management of Electronic Devices: A Review. *Nanomaterials* 10, 448–461. doi:10.3390/nano10030448

Shin, W., Cho, W., and Baik, S. J. (2018). Silver Nanowires Network Encapsulated by Low Temperature Sol-Gel ZnO for Transparent Flexible Electrodes with Ambient Stability. *Mat. Res. Express* 5, 2–21. doi:10.1088/2053-1591/aaa67a

Shinde, M. A., Mallikarjuna, K., Noh, J., and Kim, H. (2018). Highly Stable Silver Nanowires Based Bilayered Flexible Transparent Conductive Electrode. *Thin Solid Films* 660, 447–454. doi:10.1016/j.tsf.2018.06.054

Song, H., Liu, J., Liu, B., Wu, J., Cheng, H.-M., and Kang, F. (2018). Two-Dimensional Materials for Thermal Management Applications. *Joule* 2, 442–463. doi:10.1016/j.joule.2018.01.006

Tan, W. C., Saw, L. H., Yusof, F., Thiam, H. S., and Xuan, J. (2020). Investigation of Functionally Graded Metal Foam Thermal Management System for Solar Cell. *Int. J. Energy Res.* 44, 9333–9349. doi:10.1002/er.4896

Wan, Y., Zhu, X., Huang, Z., Peng, M., and Luo, H. (2021). Incorporation of Dual Nanoplatelets to a Natural Polymer for Foldable, Robust, Bioactive, and Biocompatible Nacre-like Nanocomposites. *Compos. Part B Eng.* 214, 108747. doi:10.1016/j.compositesb.2021.108747

Wei, Z., and Xu, X. (2021). Gradient Design of Bio-Inspired Nacre-like Composites for Improved Impact Resistance. *Compos. Part B Eng.* 215, 108830. doi:10.1016/j.compositesb.2021.108830

Wojtoniszak, M., and Mijowska, E. (2012). Controlled Oxidation of Graphite to Graphene Oxide with Novel Oxidants in a Bulk Scale. *J. Nanopart Res.* 14. doi:10.1007/s11051-012-1248-z

Wu, B., Chen, M., Wu, Y., Chen, Z., Xu, Z., Lu, M., et al. (2019). Fabrication and Characteristics of Cellulose Nanofibrils/Reduced Graphene Oxide Transparent Conductive Films. *J. For. Eng.* 4, 106–112.

Wu, J., Wang, L., Shan, X., and Wang, X. (2021). Preparation of 3D-W/rGO Conductive Materials by Hot-Pressing Reduction Method. *J. For. Eng.* 6, 84–93.

Xiang, C., Wang, W., Zhu, Q., Xue, D., Zhao, X., Li, M., et al. (2020). Flexible and Super-sensitive Moisture-Responsive Actuators by Dispersing Graphene Oxide into Three-Dimensional Structures of Nanofibers and Silver Nanowires. *ACS Appl. Mat. Interfaces* 12, 3245–3253. doi:10.1021/acsami.9b20365

Xiong, J., Li, S., Ye, Y., Wang, J., Qian, K., Cui, P., et al. (2018). A Deformable and Highly Robust Ethyl Cellulose Transparent Conductor with a Scalable Silver Nanowires Bundle Micromesh. *Adv. Mat.* 30, 1802803. doi:10.1002/adma.201802803

Yang, N., Zhang, Y., Jiang, J., Liu, L., and Duan, J. (2021). Preparation and Characterization of PAM/PEGDA Phase Change Energy Storage Conductive Wood Films. *J. For. Eng.* 6, 89–95.

Yang, S.-B., Choi, H., Lee, D. S., Choi, C.-G., Choi, S.-Y., and Kim, I.-D. (2015). Improved Optical Sintering Efficiency at the Contacts of Silver Nanowires Encapsulated by a Graphene Layer. *Small* 11, 1293–1300. doi:10.1002/smll.201402474

Yang, Y., Chen, S., Li, W., Li, P., Ma, J., Li, B., et al. (2020). Reduced Graphene Oxide Conformally Wrapped Silver Nanowire Networks for Flexible Transparent Heating and Electromagnetic Interference Shielding. *ACS Nano* 14, 8754–8765. doi:10.1021/acsnano.0c03337

Zhang, J., Yang, H., Shen, G., Cheng, P., Zhang, J., and Guo, S. (2010). Reduction of Graphene Oxide Vial-Ascorbic Acid. *Chem. Commun.* 46, 1112–1114. doi:10.1039/b917705a

Zhang, Q., Di, Y., Huard, C. M., Guo, L. J., Wei, J., and Guo, J. (2014). Highly Stable and Stretchable Graphene-Polymer Processed Silver Nanowires Hybrid Electrodes for Flexible Displays. *J. Mat. Chem. C* 3, 1528–1536. doi:10.1039/C4TC02448F

Zheng, C., Zhu, S., Lu, Y., Mei, C., Xu, X., Yue, Y., et al. (2020). Synthesis and Characterization of Cellulose Nanofibers/polyacrylic Acid-Polyacrylamide Double Network Electroconductive Hydrogel. *J. For. Eng.* 5, 93–100.

Zhou, L., Zhou, H., Li, J., Tan, S., Chen, P., and Xu, Z. (2019). Preparation and Properties of Nanocellulose-Based Oil -absorbing Aerogels. *J. For. Eng.* 4, 67–73.

Zhu, Y., Wan, T., Guan, P., Wang, Y., Wu, T., Han, Z., et al. (2020). Improving Thermal and Electrical Stability of Silver Nanowire Network Electrodes through Integrating Graphene Oxide Intermediate Layers. *J. Colloid Interface Sci.* 566, 375–382. doi:10.1016/j.jcis.2020.01.111

Zou, X., Zhao, M., Shen, K., Huang, C., Wu, Y., and Fang, G. (2022). Cellulose Wrapped Silver Nanowire Film with Enhanced Stability for Transparent Wearable Heating and Electromagnetic Interference Shielding. *J. Alloys Compd.* 907, 164360. doi:10.1016/j.jallcom.2022.164360

Conflict of Interest: The authors declare that the research was conducted in the absence of any commercial or financial relationships that could be construed as a potential conflict of interest.

Publisher's Note: All claims expressed in this article are solely those of the authors and do not necessarily represent those of their affiliated organizations, or those of the publisher, the editors, and the reviewers. Any product that may be evaluated in this article, or claim that may be made by its manufacturer, is not guaranteed or endorsed by the publisher.